C. T.-C. Nguyen, "High-*Q* micromechanical oscillators and filters for communications," *Proceedings* of the 1997 IEEE International Symposium on Circuits and Systems, Hong Kong, June 9-12, 1997, pp. 2825-2828.

High-*Q* Micromechanical Oscillators and Filters for Communications

Clark T.-C. Nguyen

Center for Integrated Sensors and Circuits
Department of Electrical Engineering and Computer Science
University of Michigan
2406 EECS Bldg., 1301 Beal Ave., Ann Arbor, Michigan 48109-2122, email: ctnguyen@eecs.umich.edu

ABSTRACT

With *Q*'s in the tens to hundreds of thousands, micromachined vibrating resonators are proposed as IC-compatible tanks for use in the low phase noise oscillators and highly selective filters of communications systems. To date, LF oscillators have been fully integrated using merged CMOS+microstructure technologies, and bandpass filters consisting of coupled resonators have been demonstrated in the HF range. The performance of fabricated two- and three-resonator filters with center frequencies ranging from 300kHz to 10 MHz and filter *Q*'s from 100 to 2400 are reported. Evidence suggests that the ultimate frequency range of this high-*Q* tank technology depends upon material limitations, as well as design constraints—in particular, to the degree of electromechanical coupling achievable in micro-scale resonators.

I. INTRODUCTION

The majority of the high-*Q* bandpass filters commonly used in the RF and IF stages of heterodyning transceivers are realized using off-chip, mechanically-resonant components, such as crystal filters and SAW devices. Due to higher quality factor *Q*, such technologies greatly outperform comparable filters implemented using transistor technologies, in insertion loss, percent bandwidth, and achievable rejection [2]. High *Q* is further required to implement local oscillators or synchronizing clocks in transceivers, both of which must satisfy strict phase noise specifications. Again, off-chip elements (e.g., quartz crystals) are utilized for this purpose. Being off-chip components, the above mechanical devices must interface with integrated electronics at the board level, and this constitutes an important bottleneck to miniaturization and performance of heterodyning transceivers. For this reason, recent attempts to achieve single-chip transceivers for paging and cellular communications have utilized direct conversion architectures, rather than heterodyning, and have suffered in overall performance as a result [1]. In this respect, single-chip solutions to heterodyning transceivers are desirable.

The rapid growth of micromachining technologies, which yield high-*Q* on-chip vibrating mechanical resonators [3], may now make miniaturized, single-chip heterodyning transceivers possible. With *Q*'s of over 80,000 [4] under vacuum and center frequency temperature coefficients in the range of -10 ppm/^{o}C (several times less with nulling techniques) [5], polycrystalline silicon micromechanical resonators (abbreviated "μresonators") can serve well as miniaturized substitutes for crystals in a variety of high-*Q* oscillator and filtering applications. To date, LF (i.e., 20 kHz) oscillators [6] and two-resonator prototypes of bandpass filters in the HF range have been demonstrated [7,11,12]. For use in cellular communications, however, much higher frequencies must be achieved. This paper presents an overview

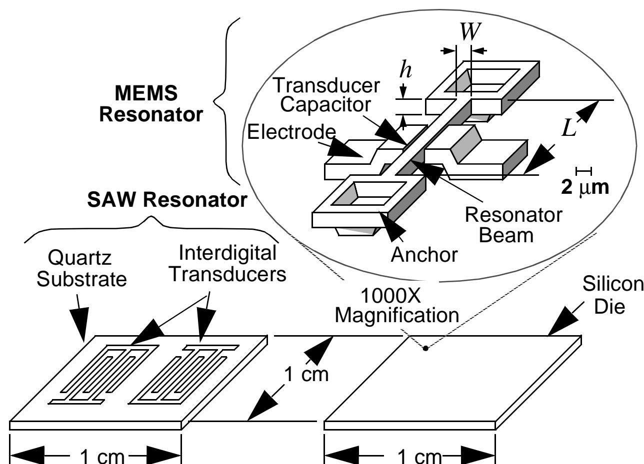

Fig. 1: Size comparison between present-day SAW resonator technology and the described high-*Q* μmechanical resonator technology.

of present efforts aimed at both size reduction and performance enhancement of transceivers via miniaturization of high-*Q* signal processing elements. Specific results will be reported, including a review of integrated oscillator work and of recently demonstrated micromechanical resonators and filters in the HF range. The remainder of this paper then focuses upon projections for the ultimate frequency range and performance of these communications devices.

II. ADVANTAGES OF MEMS

Reduced size constitutes the most obvious incentive for replacing SAW's and ceramics by equivalent μmechanical devices. The substantial size difference between micromechanical resonators and their macroscopic counterparts is illustrated in Fig. 1, which compares a typical SAW resonator with a clamped-clamped beam micromechanical resonator [7] of comparable frequency. The particular μresonator shown is excited electrostatically via parallel-plate capacitive transducers and designed to vibrate in a direction parallel to the substrate with a frequency determined by material properties, geometric dimensions, and stress in the material. Typical dimensions for a 100 MHz micromechanical resonator are $L\approx 12.9$ μm, W=2 μm, and h=2 μm. With electrodes and anchors, this device occupies an area of 420 μm^2 = 0.00042 mm^2. Compared with the several mm^2 required for a typical VHF range SAW resonator, this represents several orders of magnitude in size reduction.

A related incentive for the use of micromechanics is integrability: Micromechanical structures can be fabricated using the same planar process technologies used to manufacture integrated circuits. Several technologies demonstrating the merging of CMOS with surface micromachining have

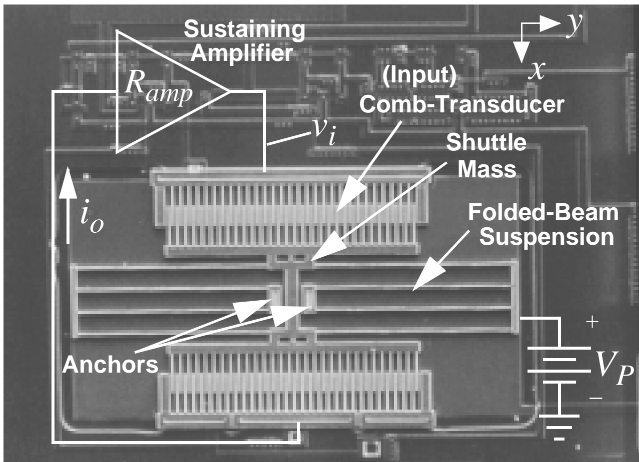

Fig. 2: SEM of a 16.5 kHz CMOS μresonator oscillator with schematics explicitly depicting circuit topology. The μresonator occupies 420 × 230 μm^2

emerged in recent years [6,8,9], and one of these is now used for high volume production of commercial accelerometers [8]. Using similar technologies, complete systems containing integrated micromechanical filters and oscillator tanks, as well as sustaining and amplification electronics, all on a single chip, are possible. This in turn makes possible high-performance, single-chip transceivers, with heterodyning architectures and all the communication link advantages associated with them. Other advantages inherent with integration are also obtained, such as elimination of board-level parasitics that could otherwise limit filter rejections and distort their passbands.

III. MEMS COMPONENTS FOR TRANSCEIVERS

The front-end of a wireless transceiver typically contains a good number of off-chip, high-Q components that are potentially replaceable by micromechanical versions. Among the components targeted for replacement are RF filters, including image rejection filters, with center frequencies ranging from 800 MHz to 2.5 GHz; IF filters, with center frequencies ranging from 455 kHz to 254 MHz; and high-Q, low phase noise oscillators, with frequency requirements in the 10 MHz to 2.5 GHz range.

Micromechanical Resonator Oscillators.

The scanning electron micrograph (SEM) for a 16.5 kHz micromechanical resonator oscillator, fully integrated with sustaining CMOS electronics, is shown in Fig. 2 [6]. To maximize frequency stability [10], a folded-beam, comb-transduced micromechanical resonator is utilized [3]. As shown, this μresonator consists of a finger-supporting shuttle mass suspended 2 μm above the substrate by folded flexures, which are anchored to the substrate at two central points. The shuttle mass is free to move in the x-direction indicated, parallel to the plane of the silicon substrate, with a fundamental resonance frequency determined largely by material properties and by geometry [3]. To properly excite this device, a voltage consisting of a dc-bias V_P and an ac excitation v_i is applied across one of the resonator-to-electrode comb-capacitors (i.e., the input transducer). This creates a force component between the electrode and resonator proportional to the product $V_P v_i$ and at the frequency of v_i. When the frequency of v_i nears its resonance frequency, the μresonator begins to vibrate, creating a dc-biased time-varying capacitor $C_o(x,t)$ at the output transducer. A current given by

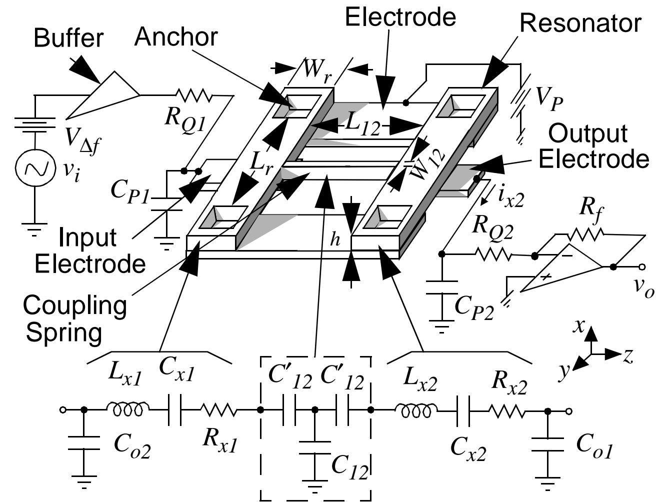

Fig. 3: Perspective view schematic of the two-resonator μmechanical filter, along with the preferred bias, excitation, and sensing circuitry, and the equivalent circuit for the filter.

$$i_o = V_P \frac{\partial C_o}{\partial x} \frac{\partial x}{\partial t} \quad (1)$$

is then generated through the output transducer, which is then amplified by the transresistance sustaining amplifier and directed back to the input comb-transducer, completing the positive feedback loop required for oscillation. The transconductance behavior of the μmechanical resonator can be modeled by an LCR equivalent circuit [6,7] when designing this oscillator.

The total area consumed by the oscillator of Fig. 2 is 420 × 330 μm^2. The measured phase noise floor of this oscillator is consistent with that of high-Q, communications-grade oscillators [6].

Micromechanical Filters.

Figure 3 presents the perspective view of a two-resonator, HF micromechanical filter, along with the preferred bias, excitation, and sensing circuitry. As shown, the filter consists of two μmechanical clamped-clamped beam resonators, coupled mechanically by a soft spring, all suspended 0.1 μm above the substrate. Conductive (polysilicon) strips underlie the central regions of each resonator and serve as capacitive transducer electrodes positioned to induce resonator vibration in a direction perpendicular to the substrate. The resonator-to-electrode gaps are determined by the thickness of a sacrificial oxide spacer during fabrication and can thus be made quite small (e.g., 0.1 μm or less), to maximize electromechanical coupling.

Under normal operation, the device is excited capacitively by a signal voltage applied to the input electrode. The output is taken at the other end of the structure, also via capacitive transduction. Upon application of an input with suitable frequency, the constituent resonators begin to vibrate in one or more flexural modes in a direction perpendicular to the substrate. For a properly designed mechanical filter, if the excitation voltage has a frequency within the passband, both resonators will vibrate. Vibration of the output resonator then couples to the output electrode, providing an output current i_{x2} given by an equation similar to (1), with x now representing displacement perpendicular to the substrate. The current i_{x2} is then directed to resistor R_{Q2}, which provides the proper

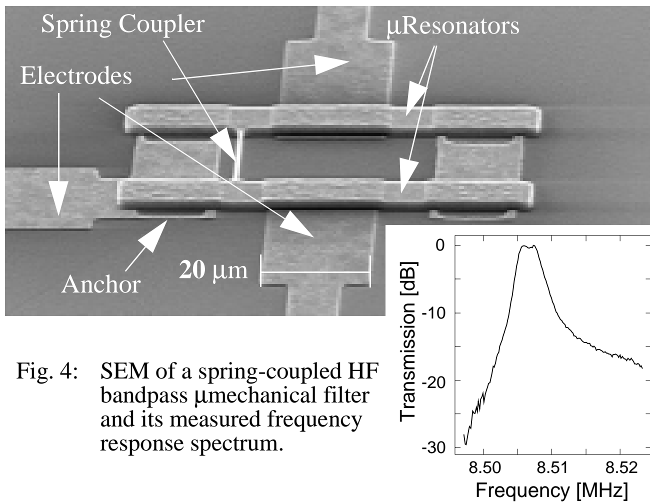

Fig. 4: SEM of a spring-coupled HF bandpass μmechanical filter and its measured frequency response spectrum.

termination impedance for the μmechanical filter. R_{Q2} then feeds a transresistance amplifier which amplifies i_{x2} to a buffered output voltage v_o.

If each resonator is designed to have the same resonance frequency, then the center frequency of the overall filter will be at this frequency. The coupling spring acts to pull the resonator frequencies apart, creating two closely spaced resonance modes that constitute the filter passband. Thus, the center frequency of a mechanical bandpass filter is determined mainly by the geometry of the constituent resonators, while its bandwidth is determined by the coupling spring(s). To properly design the resonator and coupling spring topologies, electromechanical analogies are used, where the electrical domain inductance and capacitance of a properly synthesized LC ladder filter are implemented via analogous values of compliance and mass in the mechanical domain. In effect, a mechanical ladder network (using resonators and coupling springs) is designed to match a synthesized LC filter network. Figure 3 explicitly depicts this electrical to mechanical equivalence. As shown, resonators in the mechanical domain equate to LCR tanks in the electrical domain, while coupling springs are analogous to coupling capacitors.

The SEM for an 8.5 MHz, two-resonator, prototype micromechanical filter constructed of phosphorous-doped polysilicon is shown in Fig. 4, along with a measured transmission spectrum. The center frequency for this filter is 8.5 MHz, with a bandwidth of 3.6 kHz, corresponding to an overall filter Q of 2,360.

In order to satisfy the stopband rejection requirements of most transceivers, higher order filters are required. Higher order mechanical filters can be achieved by coupling together a larger number of resonators, with the order of the bandpass filter being related to the number of resonators used. The design of such high order filters is complicated by the finite masses of the coupling beams, which can add unequally to the masses of the center and end resonators, causing mismatches in the resonance frequencies of the constituent resonators, and resulting in distortion of the filter passband. Special design strategies that cancel out the finite mass of coupling springs are required, such as designing coupling springs so that their lengths correspond to a quarter wavelength at passband frequencies [11,12], and locating coupling springs at low velocity points on the connected resonators [11,12]. These two techniques have proven very effective in suppressing finite mass phenomena and are key to achieving micro-scale mechanical filters [11,12].

Figure 5 presents the SEM of a 360 kHz, three-resonator micromechanical bandpass filter, identifying key components. The measured transmission spectrum for this filter is also shown in Fig. 5(a) and compared with the spectrum for a two-resonator filter, shown in Fig. 5(b). Note the larger stopband rejection (by ~30 dB) achieved by the higher order three-resonator filter.

IV. FREQUENCY RANGE OF APPLICABILITY

The ultimate frequency range of the described micromechanical resonators is of great interest and is presently a topic under intense study. From a purely geometric standpoint, the frequency range of micromechanical resonators can extend well into the gigaHertz range. For example, the dimensions of a clamped-clamped beam resonator required to attain a frequency of 1 GHz are (referring to Fig. 1) approximately $L \approx 4$ μm, $W = 2$ μm, and $h = 2$ μm, where finite-element analysis should be used to account for width and anchoring effects. This frequency can also be attained by longer beams vibrating in higher modes. Thus, according to analytical and finite element prediction, frequencies into the gigaHertz range are geometrically possible.

Geometry, however, is only one of many important considerations. The applicable frequency range of micromechanical resonators will also be a function of several other factors, including:

(1) quality factor, which may change with frequency for a given material, depending upon frequency-dependent energy loss mechanisms [13];

(2) series motional resistance R_x (c.f., Fig. 3), which must be minimized to suppress input-referred noise and alleviate filter passband distortion due to parasitics [7];

(3) absolute and matching tolerances of resonance frequencies, which will both be functions of the fabrication technology and of frequency trimming or tuning strategies; and

(4) stability of the resonance frequency against temperature variations, mass loading, aging, and other environmental phenomena.

Each of the above phenomena are currently under study. In particular, assuming adequate vacuum can be achieved, the ultimate quality factor will be strongly dependent upon the material type, and even the manufacturing process. For example, surface roughness or surface damage during fabrication may play a role in limiting quality factor. In fact, preliminary results comparing the quality factor achievable in boron-source-doped polysilicon structures (which exhibit substantial pitting of the poly surface) versus $POCl_3$-doped ones, indicate that the latter exhibit almost an order of magnitude higher Q at frequencies near 10 MHz. Another loss mechanism that may become more important with increasing frequency is loss to the substrate through anchors. More balanced tuning fork designs could alleviate this mechanism.

From a design perspective, the practical frequency range is limited by electromechanical coupling, which is largest when the series motional resistance R_x is smallest. R_x, indicated in Fig. 3, is given by the expression [7]

$$R_x = \frac{\sqrt{km}}{Q V_P^2 (\partial C / \partial x)^2}, \quad (2)$$

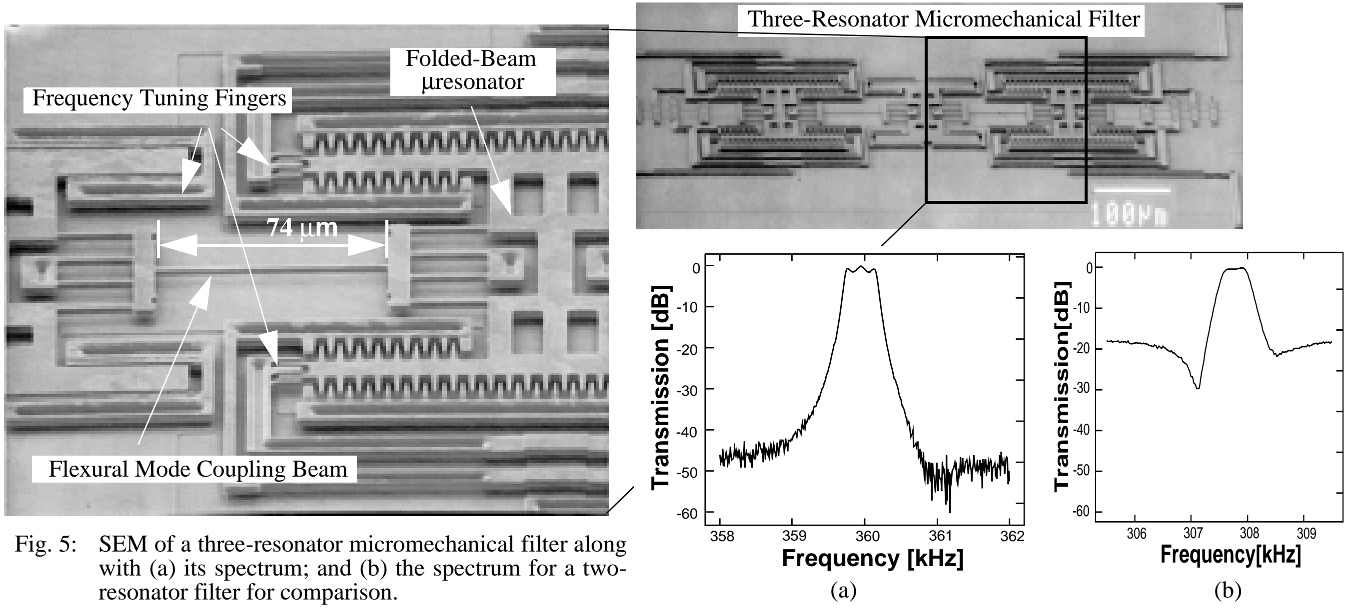

Fig. 5: SEM of a three-resonator micromechanical filter along with (a) its spectrum; and (b) the spectrum for a two-resonator filter for comparison.

where k is the system spring constant, and m is the effective mass of the resonator. Given that a frequency increase on this micro-scale often entails an increase in k with only a slight decrease in mass m, (2) suggests that R_x increases gradually with frequency. For a given frequency, R_x may be reduced by increasing the dc-bias V_P or the $\partial C/\partial x$ term. The value to which V_P may be raised is limited by the available supply voltage, or by the maximum voltage obtainable through charge-pumping. The $\partial C/\partial x$ term is proportional to the electrode-to-resonator overlap area and inversely proportional to the electrode-to-resonator gap spacing. The overlap area is limited by width effects on the resonance frequency, while the gap spacing is limited by technology. For the HF filter described above, the gap spacing is defined by an oxide spacer thickness, and thus, can be made very small, on the order of tens to hundreds of Angstroms. For this reason, the minimum gap spacing is likely not determined by process limitations, but rather by dynamic range considerations. An approximate expression for the dynamic range of the filter in Fig. 3 is

$$DR = 10\log\left[\frac{ka^2d^2}{4k_BT}\right] \qquad \text{[in dB]}\ , \tag{3}$$

where d is the electrode-to-resonator gap spacing at both input and output transducers, a is a constant determined by the magnitude of acceptable IM_3 distortion [10], k_B is the Boltzmann constant, and T is temperature. Note that DR decreases with gap spacing. On the other hand, input-referred noise, which is proportional to R_x, increases with gap spacing. Thus, for the filter design of Fig. 3 there is a trade-off between dynamic range and minimum detectable signal (*MDS*). Alternative µmechanical filter designs can be used to alleviate this situation. For example, design of the filter of Fig. 5 is influenced much less by this trade-off, because it utilizes capacitive-comb transducers, which are ideally linear over very large displacements. Due to their large mass, however, comb-transducers are less practical for high frequency designs. Alternative linearization methods are the subject of current research.

V. CONCLUSIONS

Low-phase noise oscillators and high-Q filters utilizing micromechanical vibrating resonator tanks have been demonstrated with frequencies from the LF to HF range, and requiring areas of less than 0.005 mm^2 per device on average. From a purely geometrical standpoint, the described IC-compatible mechanical resonators should be able to achieve vibrational frequencies well into the gigaHertz range. However, considerations other than geometry, such as frequency-dependent loss mechanisms, electromechanical coupling, and matching tolerances, all of which affect the ultimate performance of the described oscillators and filters, will most likely dictate the ultimate frequency range of this technology. For the case of filters, dynamic range and minimum detectable signal are found to be competing attributes in some designs. The trade-offs, however, can be made much less severe with proper design techniques.

Acknowledgments: The author gratefully acknowledges substantial contributions from former and present graduate students, in particular Frank Bannon III and Kun Wang, who are responsible for the filter results.

References:

[1] A. A. Abidi, *IEEE J. Solid-State Circuits*, vol. 30, No. 12, pp. 1399-1410, Dec. 1995.

[2] H. Khorramabadi et al., *IEEE J. Solid-State Circuits*, vol. SC-18, pp. 644-651, Dec. 1983.

[3] W. C. Tang et al., *Sensors and Actuators,* **BA21-A23**, pp. 328-331, 1990.

[4] C. T.-C. Nguyen et al., *IEDM Tech. Digest*, pp. 505-508, 1992.

[5] C. T.-C. Nguyen et al., *Transducers'93*, pp. 1040-1043, 1993.

[6] C. T.-C. Nguyen et al., *IEDM Tech. Digest*, pp. 199-202, 1993.

[7] C. T.-C. Nguyen, *Proc.*, *IEEE Int. Ultrasonics Symp.*, pp. 489-499, 1995.

[8] T. A. Core, et al., *Solid State Technology*, pp. 39-47, Oct. 1993.

[9] R. D. Nasby, et al., *Tech. Dig.*, 1996 Solid-State Sensor and Actuator Workshop, pp. 48-53, June 3-6, 1996.

[10] C. T.-C. Nguyen, Ph.D. Dissertation, 1994.

[11] F. D. Bannon III, et al., *IEDM Tech. Digest*, pp. 773-776, 1992.

[12] K. Wang, et al., *Proc.*, *IEEE MEMS Wkshp.*, pp. 25-30, 1997.

[13] V. B. Braginsky, et al., *Systems With Small Dissipation.* Univ. of Chicago Press., 1985.